Mathematics and Statistics 7(5): 158-171, 2019 http://www.hrpub.org
DOI: 10.13189/ms.2019.070502

Green's Tensor and 2Dimiensional BIE Method in Static of Massif with Arbitrary Anisotropy

Sh. A. Dildabayev*, G. K. Zakir'yanova

Institute of Mechanics and Engineering, Kazakhstan
*Corresponding Author: shdilda@bk.ru

Received August 30, 2019; Revised October 12, 2019; Accepted October 19, 2019

Abstract Up to now remains open the question of constructing fundamental solutions of the two-dimensional statics of an elastic body with arbitrary anisotropy. Also in the scope of BEM method, the question of calculating stresses in boundary points and points located close to the boundary of the region still remains actual. In this work, fundamental solutions of the static problem for elastic plane with arbitrary anisotropic properties are obtained as the sum of residues with complex variable function. The assessments of fundamental solution and theirs derivatives are presented in closed form. In the distribution space obtained are the regular representations for the Somigliana formulas and the stress calculation formulas. The numerical implementation of the BIE method in direct formulation has been realized in standard way. The test results performed for circular hole in anisotropic plane of rhombic system show a higher compliance with the boundary values of displacements and stresses and with nodes placed close to boundary. The results of analysis of the stress-strain state in the vicinity of rectangular mining chambers located deep from day surface are presented in tables and pictures of isolines.

Keywords Elastic, Anisotropy, Interior, Exterior, Boundary Value Problem, Distributions, Singular, Regular, Fundamental Solution, Convolution, Stress, Mining Chamber, Pillar

1. Introduction

The construction of fundamental solution and BEM implementation mainly for orthotropic plane domain were considered in [1-7]. Fundamental solutions for transversely isotropic magneto-electro-elastic media and boundary integral formulation where provided in [8]. The questions of justification of BEM for infinite domains were discussed in [10] for isotropic media and in [11] for orthotropic media. In [12] described the transformation technique of weakly singular and hyper singular integrals over arbitrary convex polygon into the regular contour integrals that can be easily calculated analytically or numerically.

This work is intended to show the technique to construct the fundamental solution for elastic plane with arbitrary anisotropic properties and demonstrate the ways to obtain the regular representation of singular integrals usually take place in practice of BEM method usage.

1.1. Statement of Problem

Let's consider the domain D in plane R^2 bounded by contour S, the contour may have corner nodes. For the interior problem we will consider simply connected domain inside the contour S (Fig. 1a). For exterior problem we will consider the doubly connected domain placed outside of S (Fig. 1b), where circle S_R with radius R and center at O is sufficiently large so that the region bounded by S_R covers S. In case of $R\to\infty$ we will have infinite domain with internal boundary S. Hereafter the unit outer normal is denoted by **n**.

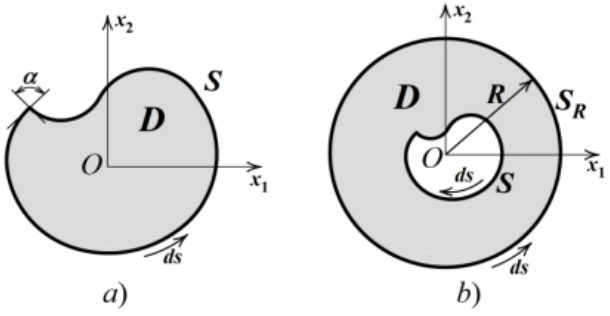

Figure 1. Interior A) And Exterior B) Problem Domains.

The differential equation of equilibrium state for homogenous anisotropic elastic body, occupied domain D, has the next form [13]

$$E_{ijkl}u_{k,lj}(\mathbf{x})+F_i(\mathbf{x})=0,\quad \mathbf{x}\in D,\quad i,j,k,l=1,2, \qquad (1)$$

where $u_i(\mathbf{x})$ are the components of displacement vector $\mathbf{u}$ in point $\mathbf{x}=(x_1,x_2)$, $F_i(\mathbf{x})$ are body force components, $\{E_{ijkl}\}$ are matrix of elasticity constants with next symmetry property $E_{ijkl}= E_{jikl} = E_{ijlk}= E_{klij}$. According to index notation the indices after comma denotes the second derivatives with respect to spatial variable x_l and x_j, and repeated index denotes summation.

The symmetry property lets present $\{E_{ijkl}\}$ matrix as 6×6 matrix $E_{\alpha\beta}$ (α,β=1,..,6). The relationship between pairs of (ij), (ml) indices and α,β indices established by next scheme (11) ↔ 1, (22) ↔ 2, (33) ↔ 3, (23)=(32)↔4, (31)=(13) ↔ 5, (31)=(13) ↔ 5.

The first and the second boundary-value problem of plane-strain elasticity is posed as follows.

Find $\mathbf{u} \in C^2(D) \cap C^1(S)$ such that (1) is satisfied in the domain D with given values of boundary displacement $f_i(\mathbf{x})$ or boundary loading $g_i(\mathbf{x})$:

$$u_i(\mathbf{x}) = f_i(\mathbf{x}), \quad \mathbf{x} \in S, \quad i=1,2, \tag{2}$$

$$E_{ijkl}u_{k,l}(\mathbf{x})n_j(\mathbf{x}) = g_i(\mathbf{x}), \quad \mathbf{x} \in S, \quad i=1,2. \tag{3}$$

2. Somigliana Formulas in Distribution Space

2.1. Basic Equation in Distributions Space

Hereafter introduce abbreviations BVP1 and BVP2 for boundary value problem (1, 2) and (1, 3) consequently. For getting solution of BVP1 and BVP2 extend functions trough all plane R^2 by entering distributions in accordance with [14]

$$\begin{aligned} \hat{u}_i(\mathbf{x}) &= H_D(\mathbf{x})u_i(\mathbf{x}), \\ \hat{F}_i(\mathbf{x}) &= H_D(\mathbf{x})F_i(\mathbf{x}), \end{aligned} \tag{4}$$

where $H_D(\mathbf{x})$ is the characteristic function of domain D. Its value in R^n (n=1,2,…) we determine according to [15]

$$H_D(\mathbf{x}) = \lim_{\varepsilon\to 0}\frac{\mu(D\cap S_\varepsilon(\mathbf{x}))}{\mu(S_\varepsilon)} = \begin{cases} 1, & \mathbf{x}\in D, \\ \alpha/(2\pi) & \mathbf{x}\in S, \\ 0, & \mathbf{x}\notin D. \end{cases} \tag{5}$$

Here $S_\varepsilon(\mathbf{x})$ is a sphere in R^n (ring for n=2) with radius ε and center in point $\mathbf{x}$, $\mu(\bullet)$- is volume (square) of region, α is an value of solid angle, formed by all kinds of tangent planes in boundary point $\mathbf{x}$ (Fig.1.a). The definition of $H_D(\mathbf{x})$ given by (5) makes possible to determine its value not only for interior and exterior points, but also for boundary points. For points on smooth part of boundary in R^n we always have $H_D(\mathbf{x})$=0.5, for points on the corner of rectangular hole in R^2 $H_D(\mathbf{x})$=0.25. So the characteristic function is always a number.

The distributions $\hat{u}_i(\mathbf{x})$, $\hat{F}_i(\mathbf{x})$ given by (5) are equal to $u_i(\mathbf{x})$ and $F_i(\mathbf{x})$ inside of D end equal to zero outside of D. Calculation second derivatives of $\hat{u}(\mathbf{x})$ with respect to spatial variables gives us next:

$$\hat{u}_{i,kj}(\mathbf{x}) = -n_j u_{i,k}(\mathbf{x})\delta_S - \partial_j\left(n_k u_i(\mathbf{x})\delta_S\right) + u_{i,kj}(\mathbf{x})H_D(\mathbf{x}), \tag{6}$$

here $n_j u_{i,k}(\mathbf{x})\delta_S$ и $\partial_j\left(n_k u_i(\mathbf{x})\delta_S\right)$ are consequently well known single layered and double layered potential distributions on contour S [14]. By using (6) we can get next expression for generalized equilibrium equation

$$E_{ijkl}\hat{u}_{k,lj}(\mathbf{x}) + \hat{F}_i(\mathbf{x}) = -E_{ijkl}n_j u_{k,l}(\mathbf{x})\delta_S - E_{ijkl}\partial_j\left(n_l u_k(\mathbf{x})\delta_S\right). \tag{7}$$

So from solving of BVP1 or BVP2 we come to find the generalized solution in D of equations (7). Solution $\hat{u}_i(\mathbf{x})$ of equation (7) in view of its definition by (4) coincides in D with solution of BVP1 or BVP2.

2.2. Green Tensor and Other Fundamental Solutions

To obtain fundamental solution of differential equations (1) we let body force component to be $F_i(\mathbf{x})= \delta_{i\beta}\delta(\mathbf{x})$, that represent concentrated force acting in x_β direction and applied in point $\mathbf{x}$, here $\delta_{i\beta}$ and $\delta(\mathbf{x})$ are Kronecker– delta and Dirac–delta. The solution for this force is entitled as Green tensor and be denoted as $U_{i\beta}(\mathbf{x})$. To construct the Green's tensor, it is convenient to use the Fourier transform, which brings the system (1) to the next system of linear equation in transform space

$$E_{ijkl}\omega_j\omega_l U^F_{k\beta}(i\omega_1, i\omega_2) = \delta_{i\beta}, \tag{8}$$

here ω_l is Fourier transform parameter. The solution of system (8) give us

$$U^F_{k\beta}(i\omega_1, i\omega_2) = \frac{Q_{k\beta}(\omega_1,\omega_2)}{Q(\omega_1,\omega_2)}, \tag{9}$$

here $Q(\omega_1, \omega_2)$ is uniform polynomial of degree 4 and represent the determinant of system (8), $Q_{k\beta}(\omega_1, \omega_2)$ are uniform polynomials of degree 2 and

$$\begin{aligned} Q_{11}(\omega_1,\omega_2) &= E_{66}\omega_1^2 + 2E_{26}\omega_1\omega_2 + E_{22}\omega_2^2, \\ Q_{12}(\omega_1,\omega_2) &= -E_{16}\omega_1^2 - (E_{12}+E_{66})\omega_1\omega_2 - E_{26}\omega_2^2, \\ Q_{22}(\omega_1,\omega_2) &= E_{11}\omega_1^2 + 2E_{16}\omega_1\omega_2 + E_{66}\omega_2^2, \\ Q(\omega_1,\omega_2) &= Q_{12}(\omega_1,\omega_2)Q_{12}(\omega_1,\omega_2) - Q_{12}^2(\omega_1,\omega_2). \end{aligned} \tag{10}$$

By using inverse Fourier transform formula we will obtain Green's tensor in Cartesian Ox_1x_2 coordinates

$$U_{kj}(\mathbf{x}) = \frac{1}{4\pi^2}\int_0^{2\pi}\int_0^{\infty}\frac{Q_{kj}(\omega_1,\omega_2)}{Q(\omega_1,\omega_2)}e^{-ix_1\omega_1 - ix_2\omega_2}d\omega_1 d\omega_2$$

Next proceed to polar coordinates $\omega_1=r\cos\alpha$, $\omega_2=r\sin\alpha$ and using uniformity of polynomials we can get

$$\begin{aligned} U_{kj}(\mathbf{x}) &= \frac{1}{4\pi^2}\int_0^{2\pi}\int_0^{\infty}\frac{Q_{kj}(\cos\alpha,\sin\alpha)}{\rho Q(\cos\alpha,\sin\alpha)}e^{-i\rho(x_1\cos\alpha + x_2\sin\alpha)}d\rho d\alpha = \\ &= \frac{-1}{4\pi^2}\int_0^{2\pi}\frac{Q_{kj}(\cos\alpha,\sin\alpha)}{Q(\cos\alpha,\sin\alpha)}\ln(x_1\cos\alpha + x_2\sin\alpha)d\alpha \end{aligned}$$

In last by introducing variable transformation z= ctgθ we obtain

$$U_{kj}(\mathbf{x}) = \frac{-1}{2\pi^2}\int_{-\infty}^{\infty} \frac{(z^2+1)Q_{kj}(z^2-1,2z)}{Q(z^2-1,2z)} \ln\left(\frac{x_1(z^2-1)}{2} + x_2 z\right) dz$$

According to the complex function theory the last integral is equal to sum of restudies of it integrand

$$U_{ki}(\mathbf{x}) = -\frac{1}{\pi^2}\sum_{p=1}^{8} res_{\mathrm{Im}\, z_p>0}\left\{\frac{(z_p^2+1)Q_{ki}(z_p^2-1,\, 2z_p)}{Q(z_p^2-1,\, 2z_p)} \times \ln\left[x_1(z_p^2-1)/2 + x_2 z_p\right]\right\}. \tag{11}$$

here z_p (p=1,…,8) are the roots of polynomial $Q(z)$ of degree 8 and in calculation are used only those that are placed in upper half plane of complex variable z. In view of logarithm is multivalued function it is necessary to remain on the same branch when traversing zeros of an expression in complex plane z

$$x_1(z_p^2-1)/2 + x_2 z_p = 0.$$

Notice that the root values of polynomial $Q(z)$ in view of (10) depend only on the elastic constants. In view of this matter, it is easy to obtain other fundamental solutions which are the derivatives of Green tensor with respect to spatial variables:

$$U_{ki,l}(\mathbf{x}) = \frac{-1}{\pi^2}\sum_{p=1}^{8} res_{\mathrm{Im}\, z_p>0}\left\{\frac{\delta_{1l}(z_p^2-1)/2 + \delta_{2l} z_p}{x_1(z^2-1)/2 + x_2 z} \times \frac{(z_p^2+1)\, Q_{ki}(z^2-1,\, 2z_p)}{Q(z^2-1,2z_p)}\right\}, \tag{12}$$

$$U_{ki,lj}(\mathbf{x}) = \frac{-1}{\pi^2}\sum_{p=1}^{8} res_{\mathrm{Im}\, z_p>0}\left\{\frac{(z^2+1)Q_{ki}(z_p^2-1,\, 2z_p)}{Q(z_p^2-1,\, 2z_p)} \times \frac{\left[\delta_{1l}(z_p^2-1)/2 + \delta_{2l} z_p\right]\left[\delta_{1j}(z_p^2-1)/2 + \delta_{2j} z_p\right]}{\left[x_1(z_p^2-1)/2 + x_2 z_p\right]^2}\right\}$$

For assessment of Green tensor and its derivatives, it is useful to present them in next form:

$$U_{ki}(\mathbf{x}) = -\frac{\ln r}{\pi^2}\sum_{p=1}^{8} res_{\mathrm{Im}\, z_p>0}\left\{\frac{(z^2+1)Q_{ki}(z_p^2-1,2z_p)}{Q(z_p^2-1,2z_p)} \ln\left[\cos\theta(z_p^2-1)/2 + \sin\theta\, z_p\right]\right\},$$

$$U_{ki,l} = \frac{-1}{\pi^2 r}\sum_{p=1}^{8} res_{\mathrm{Im}\, z_p>0}\left\{\frac{\delta_{1l}(z_p^2-1)/2 + \delta_{2l} z_p}{\cos\theta(z^2-1)/2 + \sin\theta z_p} \times \frac{(z^2+1)Q_{ki}(z^2-1,2z_p)}{Q(z^2-1,2z_p)}\right\},$$

$$U_{ki,lj} = \frac{-1}{\pi^2 r^2}\sum_{p=1}^{8} res_{\mathrm{Im}\, z_p>0}\left\{\frac{(z^2+1)Q_{ki}(z_p^2-1,2z_p)}{Q(z_p^2-1,2z_p)} \times \frac{\left[\delta_{1l}(z_p^2-1)/2 + \delta_{2l} z_p\right]\left[\delta_{1j}(z_p^2-1)/2 + \delta_{2j} z_p\right]}{\left[\cos\theta(z_p^2-1)/2 + \sin\theta\, z_p\right]^2}\right\} \tag{13}$$

$$r = \sqrt{x_1^2 + x_2^2}, \quad \cos\theta = x_1/r, \quad \sin\theta = x_2/r.$$

According to (13) for any direction $\{\cos\theta, \sin\theta\}$ on plane R^2 we have next assessments for behavior of Green tensor and its derivatives when $r \to \infty$ or $r \to 0$

$$\left|U_{k\beta}(\mathbf{x})\right| \le A\,|\ln r\,|, \quad \left|U_{k\beta,l}(\mathbf{x})\right| \le \frac{B}{r}, \quad \left|U_{k\beta,lj}(\mathbf{x})\right| \le \frac{C}{r^2} \tag{14}$$

here A, B, C are some real positive constants.

2.3. Somigliana and Stress Formulas in Distributions Space

As stated by distributions theory the convolution of Green tensor with left and right side of (7) gives its solution in next form

$$\hat{u}_i(\mathbf{x},t) = \int_S \left[U_{ki}(\mathbf{x},\mathbf{y})\, p_k(\mathbf{y}) - T_{ki}(\mathbf{x},\mathbf{y})u_k(\mathbf{y})\right]dS_y + \\ + \int_D U_{ki}(\mathbf{x},\mathbf{y})F_k(\mathbf{y})\, dV_y, \quad \mathbf{x} \in D. \tag{15}$$

In (15) we introduce next designations

$$p_k(\mathbf{x}) = u_{k,j}(\mathbf{x})n_j(\mathbf{x}), \tag{16}$$

$$T_{1i} = \left[E_{11}U_{1i,1} + E_{12}U_{2i,3} + E_{16}(U_{1i,2} + U_{2i,1})\right]n_1 + \left[E_{16}U_{1i,1} + E_{36}U_{2i,2} + E_{66}(U_{1i,2} + U_{2i,1})\right]n_2, \\ T_{2i} = \left[E_{16}U_{1i,1} + E_{26}U_{2i,2} + E_{66}(U_{1i,2} + U_{2i,1})\right]n_1 + \left[E_{12}U_{1i,1} + E_{22}U_{2i,2} + E_{36}(U_{1i,2} + U_{2i,1})\right]n_2, \tag{17}$$

here p_k are component of boundary loading, and $T_{k\beta}$ are fundamental traction tensor components generated by Green tensor, n_k components of outer normal. In view of (17) fundamental traction tensor is not symmetric tensor.

In (15) the generalized displacement in any point of D, exclude contour S, expressed by sum of integral of single layered potentials of boundary loading values p_k, double layered potential of boundary displacement values u_k and Newton potential of body force F_k.

Formula (15) is obtained for distributions. Note that in (15) on the right and on the left there are regular generalized functions for $\mathbf{x}\epsilon D$. From du Bois-Reymond's Lemma [14], it is known that every locally integrable function f defines a regular generalized function by the formula (f, φ) (φ - from the space of basic functions and contrary every regular distribution is defined by a unique locally integrable function. Due to this equation (15) are also valid in the usual sense. Similar formula for elastic media usually is obtained using Betty's theorem of the elasticity theory. The approach based on the use of distributions and performed here is more correct, since the fundamental solutions are singular distributions and to work with them it is necessary to use the same space of functions in which they are defined.

By derivation displacement given by (13) with respect to spatial variable x_i and using the elasticity Hook's law the stress formulae is obtained

$$\sigma_{km}(\mathbf{x}) = \int_S \left[D_{ikm}(\mathbf{x},\mathbf{y})\, p_i(\mathbf{y}) - V_{ikm}(\mathbf{x},\mathbf{y})u_i(\mathbf{y})\right]dS_y + \int_D W_{ikm}(\mathbf{x},\mathbf{y})F_i(\mathbf{y})\, dV_y, \quad \mathbf{x} \in D \tag{18}$$

where potentials kernel are

$$D_{i11} = E_{11}U_{i1,1} + E_{12}U_{i2,2} + E_{16}\left(U_{i1,2} + U_{i2,1}\right), \\ D_{i22} = E_{12}U_{i1,1} + E_{22}U_{i2,2} + E_{26}\left(U_{i1,2} + U_{i2,1}\right), \\ D_{i21} = E_{16}U_{i1,1} + E_{26}U_{i2,2} + E_{66}\left(U_{i1,2} + U_{i2,1}\right),. \tag{19}$$

$$V_{i11} = E_{11}T_{i1,1} + E_{12}T_{i2,2} + E_{16}\left(T_{i1,2} + T_{i2,1}\right), \\ V_{i22} = E_{12}T_{i1,1} + E_{22}T_{i2,2} + E_{26}\left(T_{i1,2} + T_{i2,1}\right), \\ V_{i21} = E_{16}T_{i1,1} + E_{26}T_{i2,2} + E_{66}\left(T_{i1,2} + T_{i2,1}\right),. \tag{20}$$

$$W_{i11} = E_{11}U_{i1,1} + E_{12}U_{i2,2} + E_{16}\left(U_{i1,2} + U_{i2,1}\right), \\ W_{i22} = E_{12}U_{i1,1} + E_{22}U_{i2,2} + E_{26}\left(U_{i1,2} + U_{i2,1}\right), \\ W_{i21} = E_{16}U_{i1,1} + E_{26}U_{i2,2} + E_{66}\left(U_{i1,2} + U_{i2,1}\right),. \tag{21}$$

So the Somigliana formula give the solution of BVP1 or BVP2 thereat for BVP1 we have Fredholm equations of first kind, and second kind for BVP2 when $\mathbf{x}\epsilon S$.

2.4. Gauss Formula and Regular Presentation of Somigliana and Stress Formulas

In view of assessments (14), for Green tensor and its derivatives, the potential kernels $T_{i\beta}(\mathbf{x},\mathbf{y})$ in Somigliana formulas and potential kernels $D_{ikj}(\mathbf{x},\mathbf{y})$, $V_{ikj}(\mathbf{x},\mathbf{y})$ has singularities on contour S when $\mathbf{x}=\mathbf{y}$. For performing, the regular presentation of (14) is used Gauss formula for double-layered potential. In this objection, lets take convolution of characteristic function $H_D(\mathbf{x})$ (5) of finite domain D with equilibrium equation for concentrated body force

$$E_{ijkl}U_{\beta k,lj}(\mathbf{x}) + \delta_{i\beta}\delta(\mathbf{x}) = 0, \quad \mathbf{x} \in R^2.$$

Performing convolution with first term gives

$$\int_{R^2} E_{ijkl}U_{\beta k,lj}(\mathbf{x}-\mathbf{y})H_D(\mathbf{x})dV_y = \int_D E_{ijkl}U_{\beta k,lj}(\mathbf{x}-\mathbf{y})dV_y = \int_S E_{ijkl}U_{\beta k,l}(\mathbf{x}-\mathbf{y})n_j(\mathbf{y})dS_y = \int_S T_{i\beta}(\mathbf{x}-\mathbf{y})dS_y = \overline{T}_{i\beta}(\mathbf{x})$$

In last expression on pass from body integral to contour integral the Gauss formula is used. Convolution with second terms gives

$$\int_{R^2} H_D(\mathbf{x})\delta_{i\beta}\delta(\mathbf{x}-\mathbf{y})dV_y = \delta_{i\beta}\int_D \delta(\mathbf{x}-\mathbf{y})dV_y = \delta_{i\beta}H_D(\mathbf{x})$$

Finally, for double potential kernel $T_{i\beta}$ we obtain the Gauss formulas for finite domain D with finite contour

$$\overline{T}_{i\beta}(\mathbf{x}) = \int_S T_{i\beta}(\mathbf{x},\mathbf{y})\,dS_y = -\delta_{i\beta}H_D(\mathbf{x}) \tag{21}$$

For infinite domain consider the doubly connected domain D placed outside of S (Fig. 1b), where circle S_R with finite radius R with center at O is sufficiently large so that the region bounded by S_R covers S. For this finite domain we have

$$\overline{T}_{i\beta}(\mathbf{x}) = \int_{S\cup S_R} T_{i\beta}(\mathbf{x},\mathbf{y})\,dS_y = -\delta_{i\beta}H_D(\mathbf{x})$$

or

$$\int_S T_{i\beta}(\mathbf{x},\mathbf{y})\,dS_y + \int_{S_R} T_{i\beta}(\mathbf{x},\mathbf{y})\,dS_y = -\delta_{i\beta}H_D(\mathbf{x})$$

For finite contour S_R with arbitrary large radius R integral of double potential with kernel $T_{i\beta}$ in view of (21) is equal to $-\delta_{i\beta}H_D(\mathbf{x})$ and we have

$$\int_S T_{i\beta}(\mathbf{x},\mathbf{y})\,dS_y - \delta_{i\beta}H_D(\mathbf{x}) = -\delta_{i\beta}H_D(\mathbf{x})$$

And as the last equality is valid for arbitrary contour of large diameter R so it also valid for $R\to\infty$ and finally we have Gauss formula for infinite domain outside of S

$$\overline{T}_{i\beta}(\mathbf{x}) = \int_S T_{i\beta}(\mathbf{x},\mathbf{y})\,dS_y = (1-H_D(\mathbf{x}))\delta_{i\beta}, \tag{22}$$

Gauss formula is important in applications because it gives simply and obvious geometric representation to get the values of double layered potential of fundamental traction tensor and to verify its numerical implementation. The direct numerical calculations for Gauss formulae were implemented and the results are presented in next section.

Using Gauss formulae we can obtain the regular representation of Somigliana formulas. By adding to (15) Gauss formulas (21) multiplied on $u_k(\mathbf{x})$ in case when $\mathbf{x}\in D$ we have next expression

$$(1-H_D(\mathbf{x}))u_i(\mathbf{x}) = \int_S \{U_{ki}(\mathbf{x},\mathbf{y})p_k(\mathbf{y}) - T_{ki}(\mathbf{x},\mathbf{y})(u_k(\mathbf{y})-u_k(\mathbf{x}))\}dS_y + \int_D U_{ki}(\mathbf{x},\mathbf{y})F_k(\mathbf{y})\,dV_y, \quad x\in D. \tag{23}$$

In view definition (5) of $H_D(\mathbf{x})$ the left side of (23) for interior BVP equal to zero and for exterior problems the left side is equal to $u_\beta(\mathbf{x})$. In this representation when integration point $\mathbf{y}$ is very close to $\mathbf{x}$ ($\mathbf{x}$ in domain or on contour) we have integrable singularity.

In case $\mathbf{x}\in S$ the expression (23) becomes boundary integral equation (BIE), and exclusion of singularity in this manner is very useful during numerical solution of BIE.

By derivation displacement given by (23) with respect to spatial variable x_i and using Hook's law the regular representation of stress formulae is obtained

$$\begin{aligned}\sigma_{kq}(\mathbf{x}) = &\int_S [D_{ikq}(\mathbf{x},\mathbf{y})p_i(\mathbf{y}) - V_{ikq}(\mathbf{x},\mathbf{y})(u_k(\mathbf{y})-u_k(\mathbf{x}))]dS_y + \\ &+\sigma_{iq}(\mathbf{x})\int_S T_{i\beta}(\mathbf{x},\mathbf{y})\,dS_y + \int_D W_{ikq}(\mathbf{x},\mathbf{y})F_i(\mathbf{y})\,dV_y, \quad \mathbf{x}\in D.\end{aligned} \tag{24}$$

In case when $\mathbf{x}\in S$ we have next regularized formula for boundary stress calculation

$$\sigma_{km}(\mathbf{x}) = \frac{1}{1-H_D(\mathbf{x})+\alpha/(2\pi)}\left\{\int_S \left[D_{ikm}(\mathbf{x},\mathbf{y})\,p_i(\mathbf{y}) - V_{ikm}(\mathbf{x},\mathbf{y})\times\right.\right.$$
$$\left.\left.\times\left(u_k(\mathbf{y})-u_k(\mathbf{x})\right)\right]dS_y + \int_D W_{ikm}(\mathbf{x},\mathbf{y})F_i(\mathbf{y})\,dV_y\right\}, \quad \mathbf{x}\in S, \tag{25}$$

where $H_D(\mathbf{x}) = 1$ for interior BVP of finite regions, and $H_D(\mathbf{x}) = 1$ for exterior BVP of infinite domain.

3. Numerical Implementation and Test Results

3.1. Discrete Analogues of Somigliana and Stress Formulas

The numerical implementation of the BIE method in direct formulation has been realized in standard way. The boundary contours of region were approximated by the finite set of $\{S_l\}$ (l = 1, L) of 3-nodal isoperimetric quadrilateral elements (See Fig 2.). The nodes of all elements and regional nodes form some finite set of nodes ordered by continuous numbering. In accordance with this, each boundary node will have a unique global number in set and local number on element. In follows we will use upper indexing for the node values of the desired and given functions $f_i^k = f_i(\mathbf{x}^k)$.

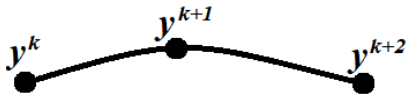

Figure 2. 3-Nodal Quadrilateral Isoperimetric Element

The Cartesian coordinates y_i of an arbitrary point of the element S_k, and the values of the functions at this point are parametrically expressed in terms of the node values using the form functions of the local coordinates $\boldsymbol{\zeta}=(\zeta_1, \zeta_2)$ in form of relations:

$$y_i(\xi) = \sum_{k=1}^{3} L^k(\xi)\,y_i^{\varphi(l,k)}, \qquad |\,\xi\,| \le 1,$$
$$f_i(\xi) = \sum_{k=1}^{3} L^k(\xi)\,f_i^{\varphi(l,k)}, \qquad |\,\xi\,| \le 1, \tag{26}$$

here $\varphi(l,k)$ is the global number of the node having the local number k in the l–th element, $L_k(\xi)$ are form-functions of isoperimetric element

$$L^1(\xi) = 0.5\xi(\xi-1),$$
$$L^2(\xi) = -(\xi+1)(\xi-1), \tag{27}$$
$$L^3(\xi) = 0.5\xi(\xi+1).$$

The discrete analogues of regularized boundary integral equation (23) and stress formulae's (25) in assumption of absence of body force are obtained by replace contour integral by sum of integral on the elements and using interpolation (26) and form-functions(27)

$$u_i^n = \sum_{l=1}^{L}\sum_{s=1}^{3}\left[\overline{U}_{ij}^{n,s}\,p_j^{\varphi(l,s)} - \overline{T}_{ij}^{n,s}\left(u_j^{\varphi(l,s)} - u_j^n\right)\right],$$
$$\sigma_{ik}^n = \sum_{l=1}^{L}\sum_{s=1}^{3}\left[\overline{D}_{ikj}^{n,s}\,p_j^{\varphi(l,s)} - \overline{V}_{ikj}^{n,s}\left(u_j^{\varphi(l,s)} - u_j^n\right)\right], \tag{28}$$

here

$$\overline{U}_{ij}^{n,s} = \int_{-1}^{1} U_{ij}\left(\mathbf{x}^n, \mathbf{y}(\xi)\right)L^s(\xi)J(\xi)d\xi,$$
$$\overline{T}_{ij}^{n,s} = \int_{-1}^{1} T_{ij}\left(\mathbf{x}^n, \mathbf{y}(\xi)\right)L^s(\xi)J(\xi)d\xi,$$
$$\overline{D}_{ikj}^{n,s} = \int_{-1}^{1} D_{ikj}\left(\mathbf{x}^n, \mathbf{y}(\xi)\right)L^s(\xi)J(\xi)d\xi, \tag{29}$$
$$\overline{V}_{ikj}^{n,s} = \int_{-1}^{1} V_{ikj}\left(\mathbf{x}^n, \mathbf{y}(\xi)\right)L^s(\xi)J(\xi)d\xi,$$

$J(\xi)$ is the Jacobean of the transformation (26). The integrals (29) are calculated by using Gauss quadrature.

In case when the element S^l includes node $\mathbf{x}^n$ it subdivided on subelements according to technique suggested in [16].

For calculation roots of polynomials $Q(z^2+1, 2z)$ the Newton method was performed.

3.2. Compare with Analytical Solution for Exterior Problem of Infinite Domain

For verification of proposed fundamental solution and regular representation of Somigliana and stress formulas the numerical results were compared with analytical solution given in [13] for cylindrical hole with unit radius R=1 under inner pressure. Anisotropic media of rhombic system (aragonite ($CaCO_3$)) [17] is considered with elastic constants

$$E_{11}= 1.60,\ E_{22}= 0.87,\ E_{33}=0.85,\ E_{44}= 0.41,\ E_{55}= 0.26,$$
$$E_{66}= 0.43,\ E_{12}= 0.37,\ E_{13}= 0.02,\ E_{23}= 0.168 \tag{30}$$

The values of elastic constants depends on the choice of the directions of the system coordinate axes. The values of

(30) are given for the case when the directions of the principal axes of symmetry of the elastic constants coincide with the directions of the axes of global system coordinates. Next, on occasion, for indexed coordinates x_i (i=1,2,3) we use traditional symbols x, y and z consequently.

In case when the direction of global axes coordinate $Oxyz$ and the directions of symmetry axes of elastic constants $O\xi\nu\zeta$ are differ, the elastic constant values in global coordinate system are expressed by

$$C_{pqrs} = \alpha_{ip}\alpha_{jq}\alpha_{kr}\alpha_{ls}C'_{ijkl} \qquad (31)$$

here C'_{ijlk} – elastic constant values in principal symmetry axes, α_{ij}-direction cosines of principal symmetry axes in global system. In the case of two-dimensional problems, it is possible only the axes rotation in the Oxy plane relative to the origin. The rotation angle of the axes of the $O\xi\nu$ system relative to the Oxy axes will be denoted by Ω.

The numerical results are computed by solving integral equation (23) and stress calculation by (24,25) for approximation of hole with 16 and 32 of 3-nodal isoperimetric elements.

The epure of obtained circular σ_θ stress in case Ω= 0° is symmetrical about axe Oy (see Fig.2) and σ_θ values are equal to 1.4530 at θ= 0°, and 1.6206 at θ= 90°. In case Ω= 30° the epure of σ_θ stress rotated by 30°.

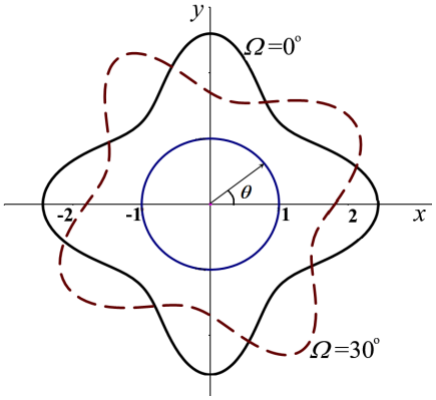

Figure 3. Circular σ_θ stresses distribution on contour of cylindrical hole for Ω= 0° and 30°.

Below in Table 1 are presented numerical and analytical results of radial displacements u_R and circular stresses σ_θ for Ω=0° in some boundary and regional nodes, placed close to hole contour on radiuses 1.005, 1.01, 1.02, 1.1 in case of contour division by L=16 and L=32 elements.

The obtained numerical results are in good agreement with analytical values even for so rough approximation of boundary contour. The numerical boundary stress values are in conform to those analytical better than the stress values for regional nodes placed concentering on radius r=1.005 and r=0.01. This indicates the extra high efficiency of calculation boundary displacement and stress values using regular representation for Somigliana (23) and stress (26) formulas.

Table 1. Comparison of numerical and analytical radial displacement u_r and angular stress σ_θ values in boundary and regional points

x	y	$u_{r\ L=16}$	u_{ran}	$\sigma_{\theta\ L=16}$	$\sigma_{\theta\ L=32}$	$\sigma_{\theta an}$
1.000	0.000	1.0160	1.0167	1.4530	1.4410	1.4393
0.924	-0.383	1.1437	1.1445	0.9982	0.9951	0.9946
0.707	-0.707	1.4050	1.4058	0.5982	0.6007	0.6010
0.000	-1.000	1.7077	1.7085	1.6206	0.1605	1.6027
1.005	0.000	1.0267	1.0135	1.3901	1.4063	1.4074
0.928	-0.385	1.1946	1.1372	0.6869	0.9611	0.9878
0.711	-0.711	1.4023	1.3970	0.5682	0.6197	0.6039
0.000	-1.005	1.7451	1.7026	1.5027	1.5478	1.5485
t1.010	0.000	1.0244	1.0103	1.3764	1.3766	1.3769
0.933	-0.387	1.1207	1.1301	0.9621	0.9813	0.9807
0.714	-0.714	1.3836	1.3882	0.6213	0.6072	0.6067
0.000	-1.010	1.7023	1.6967	1.4973	1.4982	1.4986
1.020	0.000	0.9857	0.9862	1.3192	1.3195	1.3196
0.942	-0.390	1.0772	1.0778	0.9666	0.9659	0.9660
0.721	-0.721	1.3194	1.3200	0.6125	0.6119	0.6119
0.000	-1.020	1.6514	1.6519	1.4084	1.4089	1.4092
1.100	0.000	0.9581	0.9586	0.9886	0.9888	0.9890
1.016	-0.421	1.0210	1.0215	0.8387	0.8389	0.8390
0.778	-0.778	1.2396	1.2401	0.6363	0.6364	0.6365
0.000	-1.100	1.5998	1.6003	0.9768	0.9772	0.9774

The results of direct numerical calculation of double potential integral $\overline{T}_{ij}(\mathbf{x})$ (22) for Ω=0° in case of circular contour division by 16 elements for some boundary and regional nodes are presented in Table 2. For division of contour by 16 elements obtained good agreement with Gauss formula for boundary points and regional points placed on concentering radius r=1.01 and more. The less better outcomes for points on radius r=0.05 are caused by singularity of kernel $T_{ij}(\mathbf{x})$.

Table 2. Components value of double potential integral in some boundary and regional points (L=16, Ω= 0°)

x	y	$\overline{T}_{11}$	$\overline{T}_{12}$	$\overline{T}_{12}$	$\overline{T}_{22}$
1.000	0.000	-5.04E-01	1.61E-09	-1.08E-09	-5.20E-01
0.924	-0.383	-5.04E-01	2.26E-03	4.25E-03	-5.15E-01
0.707	-0.707	-5.07E-01	3.95E-03	4.47E-03	-5.09E-01
0.383	-0.924	-5.16E-01	5.09E-03	3.38E-03	-5.06E-01
1.005	0.000	2.95E-16	-4.02E-01	0.00E+00	0.00E+00
0.929	-0.385	-2.31E-02	-4.12E-01	0.00E+00	0.00E+00
0.711	-0.711	-3.81E-02	-4.42E-01	0.00E+00	0.00E+00
0.558	-0.836	-2.95E-02	-4.85E-01	0.00E+00	0.00E+00
1.010	0.000	0.00E+00	0.00E+00	0.00E+00	0.00E+00
0.933	-0.387	0.00E+00	0.00E+00	0.00E+00	0.00E+00
0.714	-0.714	0.00E+00	0.00E+00	0.00E+00	0.00E+00
0.386	-0.933	0.00E+00	0.00E+00	0.00E+00	0.00E+00

4. Stress Strain State of Rock Massif with Rectangular Chambers

4.1. Preliminary Notes

Generally in investigation of problems of mining geomechanics the stress-strain state in the rock massive with holes is the superposition of field of initial stresses $\sigma_{ij}^0(\mathbf{x})$ in untouched massif and field of additional stresses $\sigma_{ij}^a(\mathbf{x})$ caused by presence of hole

$$\sigma_{ij}(\mathbf{x}) = \sigma_{ij}^0(\mathbf{x}) + \sigma_{ij}^a(\mathbf{x}) \tag{32}$$

The stress state of an untouched massif is determined on the hypothesis of A.N. Dinnik based on the possibility only vertical displacements in it

$$u_1^0(\mathbf{x}) = 0, \quad u_2^0(\mathbf{x}) = w(y), \quad u_3^0(\mathbf{x}) = 0. \tag{33}$$

On the assumption of (33), the next components of strain tensor are equal to zero

$$\varepsilon_{xx}^0 = \varepsilon_{xy}^0 = \varepsilon_{xz}^0 = \varepsilon_{yz}^0 = \varepsilon_{zz}^0 = 0.$$

Suppose $\sigma_{yy}^0 = -\gamma H$ -where γ –the volume weight of massif, – the depth of considered point. Using (33) and elasticity Hook's law are derived other values of stress tensor

$$\begin{aligned} &\sigma_{yy}^0 = -\gamma H, \qquad \sigma_{xx}^0 = -\lambda_x \gamma H, \qquad \sigma_{zz}^0 = -\lambda_z \gamma H, \\ &\sigma_{xy}^0 = -\lambda_{xy} H, \qquad \sigma_{xz}^0 = \sigma_{yz}^0 = 0, \end{aligned} \tag{34}$$

where

$$\lambda_x = c_{12}/c_{22}, \quad \lambda_y = c_{23}/c_{22}, \quad \lambda_{xy} = c_{26}/c_{22}$$

4.2. Stresses in Vicinity of Two Rectangular Chambers in Rock Massive

Now consider two rectangular chambers of 8m×5m of size placed on 70 m depth from the day surface with intechamber pillars width of 5m (Fig. 4). The elastic constant of massif are according to (30) for Ω=0° and (31) for Ω=30°.

The boundary contours of chambers S are free of loading

$$\sigma_{ij}(\mathbf{x}) n_j(\mathbf{x}) = 0, \quad \mathbf{x} \in S.$$

So for determination of additional stress field we have next boundary conditions on contours S

$$\sigma_{ij}^a(\mathbf{x}) n_j(\mathbf{x}) = -\sigma_{ij}^0(\mathbf{x}) n_j(\mathbf{x}), \quad \mathbf{x} \in S.$$

The numerical analysis was performed for each contour of chamber approximated by 80 quadrilateral 3–nodal elements with 320 surface nodes in total and 4726 regional nodes.

The numerical results of stress component σ_{xx}, σ_{xy}, σ_{yy} and T_I– second invariant of stress tensor are presented for elements of chamber such as pillars, roofs and floors (Fig.4).

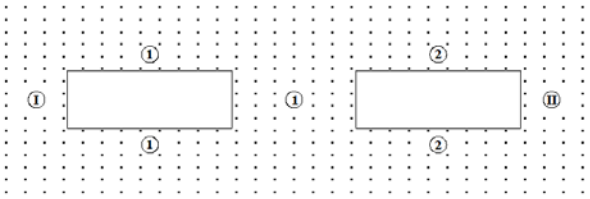

Figure 4. Two rectangular mining chambers in rock massive and their elements: I, II– barrier pillars; 1– interchamber pillar; 1, 2 – roof and floor of chambers

The most loaded element of mining are the intechamber pillar 1 and then barrier pillars I, II (see Tables 2, 3), the roofs and floors of chambers are loaded less. The interchamber pillar is loaded more 14% than barriers pillars, more 192% than roofs and 112% than floors.

Table 3. Arithmetic mean values of stresses in pillars, Roof and Floor of chambers for Ω=0°

	Pillars			Roof		Floor	
σ_{ik}\№	I	1	II	1	2	1	2
σ_{xx}	-11.4	-13.4	-11.4	1.99	1.99	1.33	1.33
σ_{xy}	0.61	0.00	-0.61	-0.85	0.85	1.30	-1.30
σ_{yy}	-122.9	-139.9	-122.9	-36.5	-36.5	-53.9	-53.9
T_I	57.1	64.9	57.1	22.2	22.2	30.6	30.6

Table 4. Arithmetic mean values of stresses in pillars, Roof and Floor of chambers for Ω=30°

	Pillars			Roof		Floor	
σ_{ik}\№	I	1	II	1	2	1	2
σ_{xx}	-13,63	-15,77	-14,4	-4,78	-5,93	-8,59	-7,38
σ_{xy}	6,32	6,99	5,39	2,86	5,05	6,66	3,57
σ_{yy}	-122,11	-140,87	-123,04	-37,51	-37,21	-54,60	-54,54
T_I	56,38	64,93	56,33	20,20	20,24	27,78	27,57

The maximal stresses of mining elements are observed in the neighbor of corners of chambers and theirs values presented in Tables 5, 6.

Table 5. Maximal values of stresses in pillars, Roof and Floor of chambers for Ω=0°

	Pillars			**Roof**		**Floor**	
σ_{ik}**\№**	**I**	**1**	**II**	**1**	**2**	**1**	**2**
σ_{xx}	-27.25	-31.60	-27.25	71.50	71.50	74.42	74.42
σ_{xy}	-24.80	28.16	-24.80	51.92	-51.92	-53.70	53.70
σ_{yy}	-203.9	-215.7	-203.9	-63.28	-63.28	-80.29	-80.29
T_I	103.1	109.1	103.1	58.30	58.30	60.69	60.69

Table 6. Maximal values of stresses in pillars, Roof and Floor of chambers for Ω=30°

	Pillars			**Roof**		**Floor**	
σ_{ik}\№	**I**	**1**	**II**	**1**	**2**	**1**	**2**
σ_{xx}	-35,01	-37,14	-30,72	-63,26	-58,73	-66,37	-68,61
σ_{xy}	37,05	40,76	35,14	62,68	57,39	61,22	65,82
σ_{yy}	-227,91	-244,53	-211,59	-76,66	-69,48	-83,08	-82,2
T_I	115,64	124,26	108,31	67,67	61,58	65,48	70,95

It is seen (Table 5, 6), that for case Ω=30° the maximal stresses value exceed the stresses for Ω=30° from 5% to 18 %..

The isolines of stresses σ_{yy} and T_I show that stress concentration are observed in points closest to chambers contour and the most concentration are around the corner of chambers (see Fig.5-6). The stress values on isolines are presented in Tables 7-10.

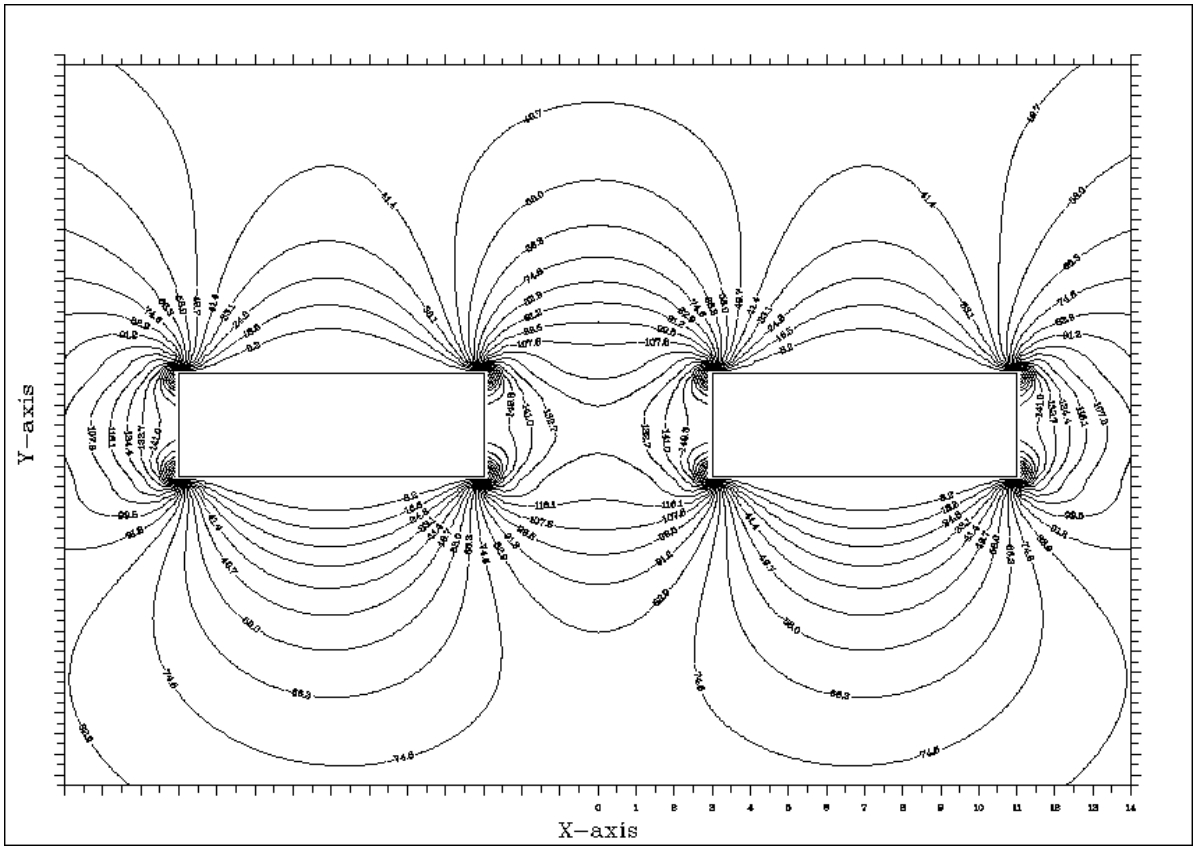

Figure 5. Isolines of stress σ_{yy} for Ω=0°

Table 7. Stress σ_{yy} value on isolines

№	σ_{yy}	№	σ_{yy}	№	σ_{yy}	№	σ_{yy}	№	σ_{yy}
1	-215.7	7	-171.1	13	-126.4	19	-81.8	25	-37.1
2	-208.3	8	-163.6	14	-118.9	20	-74.3	26	-29.7
3	-200.8	9	-156.2	15	-111.5	21	-66.9	27	-22.2
4	-193.4	10	-148.7	16	-104.1	22	-59.4	28	-14.8
5	-185.9	11	-141.3	17	-96.64	23	-52.0	29	-7.3
6	-178.5	12	-133.9	18	-89.2	24	-44.5	30	0.11

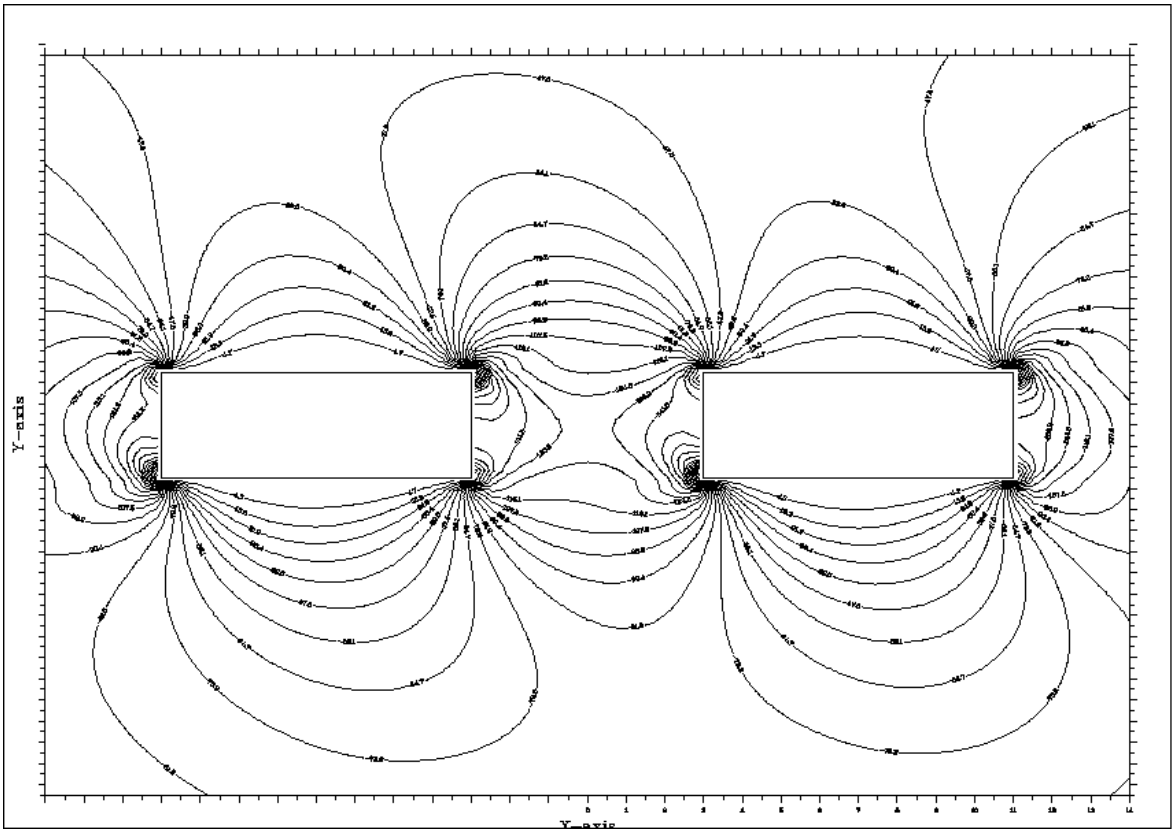

Figure 6. Isolines of stress σ_{yy} for Ω=30°

Table 8. Stress σ_{yy} value on isolines

№	σ_{yy}	№	σ_{yy}	№	σ_{yy}	№	σ_{yy}	№	σ_{yy}
1	-244,5	7	-193,2	13	-141,8	19	-90,37	25	-38,98
2	-236,0	8	-184,6	14	-133,2	20	-81,81	26	-30,42
3	-227,4	9	-176,0	15	-124,6	21	-73,24	27	-21,86
4	-218,8	10	-167,5	16	-116,1	22	-64,68	28	-13,29
5	-210,3	11	-158,9	17	-107,5	23	-56,11	29	-4,73
6	-201,7	12	-150,3	18	-98,94	24	-47,55	30	3,84

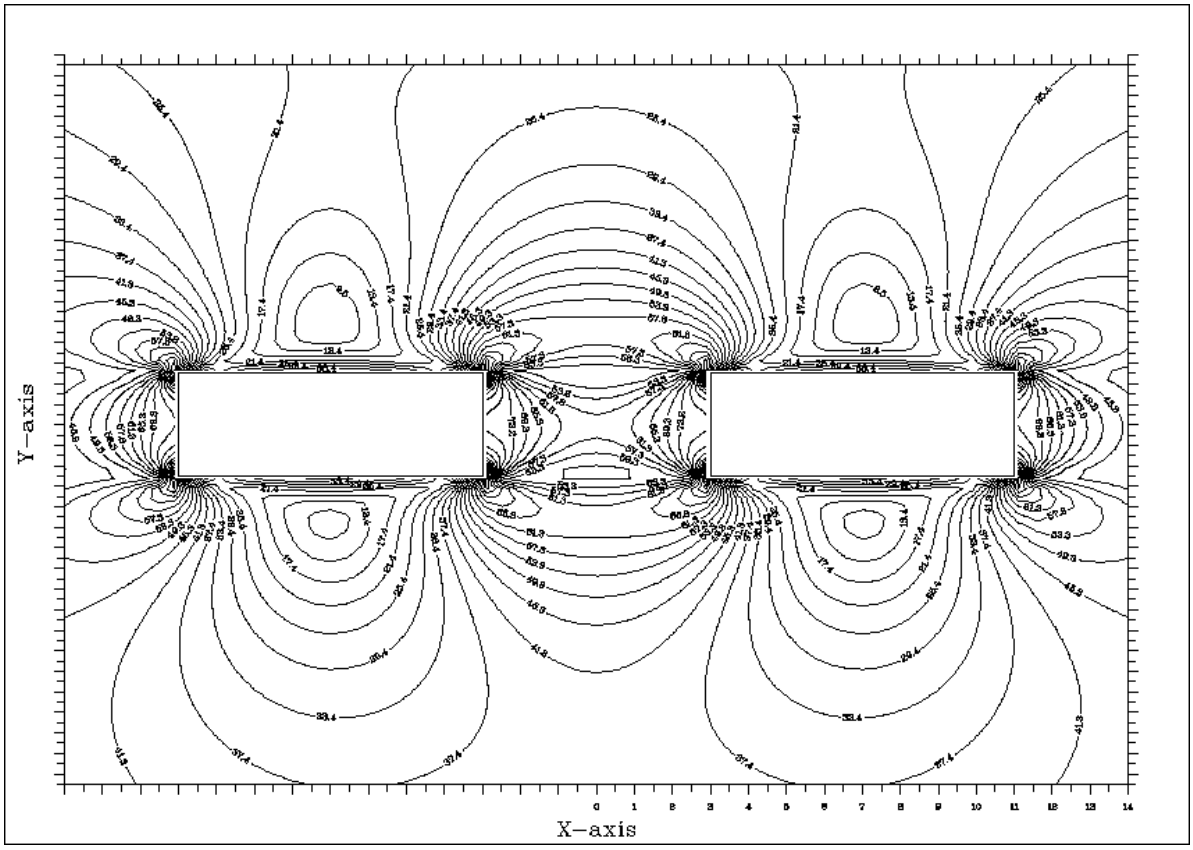

Figure 7. Isolines of stress T_I. for Ω=0°

Table 9. T_I stress value on isolines

№	T_I	№	T_I	№	T_I	№	T_I	№	T_I
1	5.47	7	26.9	13	48.36	19	69.80	25	91.3
2	9.04	8	30.5	14	51.93	20	73.38	26	94.8
3	12.6	9	34.1	15	55.51	21	76.9	27	98.4
4	16.2	10	37.6	16	59.08	22	80.5	28	101.9
5	19.9	11	41.21	17	62.65	23	84.1	29	105.5
6	23.3	12	44.78	18	66.23	24	87.7	30	109.1

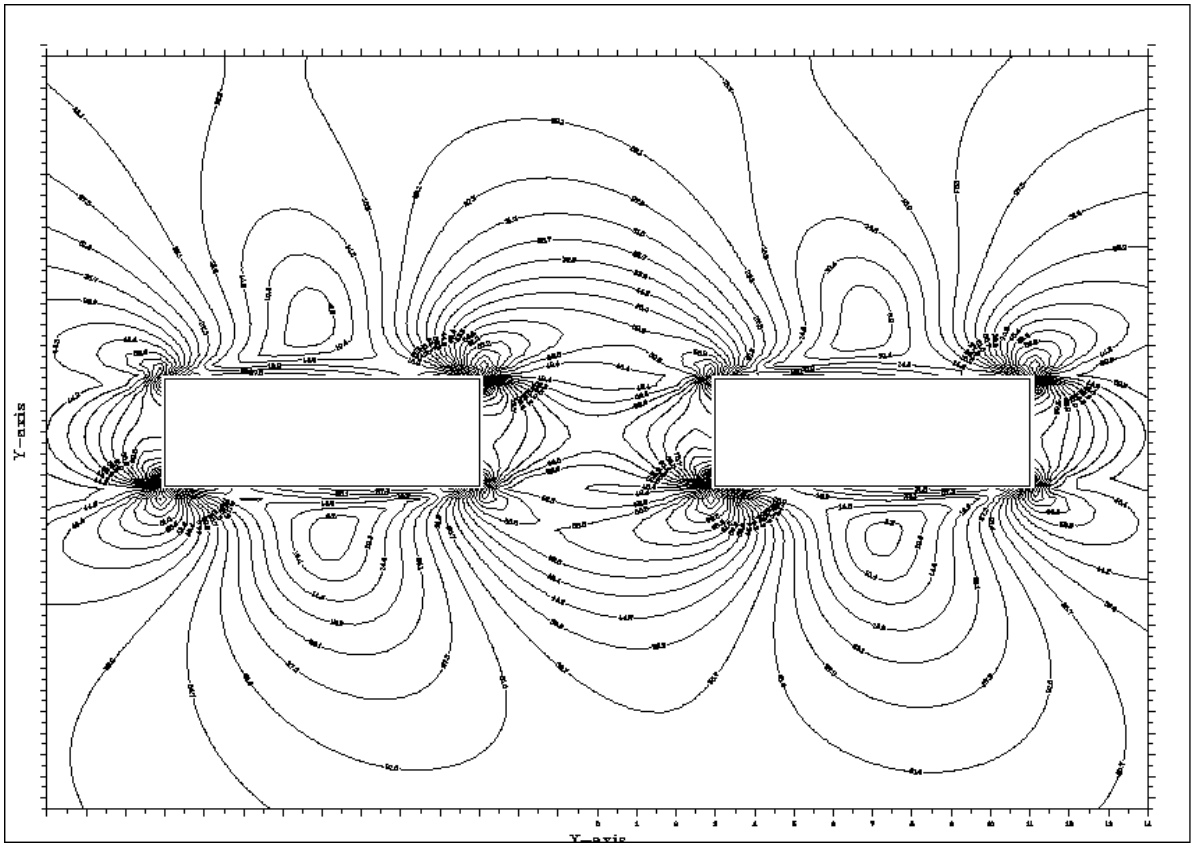

Figure 8. Isolines of stress T_I for Ω=30°

Table 10. T_I stress value on isolines

№	T_I	№	T_I	№	T_I	№	T_I	№	T_I
1	2,00	7	27,29	13	52,59	19	77,88	25	103,2
2	6,22	8	31,51	14	56,81	20	82,10	26	107,4
3	10,43	9	35,73	15	61,02	21	86,32	27	111,6
4	14,65	10	39,94	16	65,24	22	90,53	28	115,8
5	18,86	11	44,16	17	69,45	23	94,75	29	120,0
6	23,08	12	48,37	18	73,67	24	98,96	30	124,3

In case Ω=0° the stress field distribution is symmetric about the *Oy* axis (see Fig.5,7,9 and Tables 3,5).

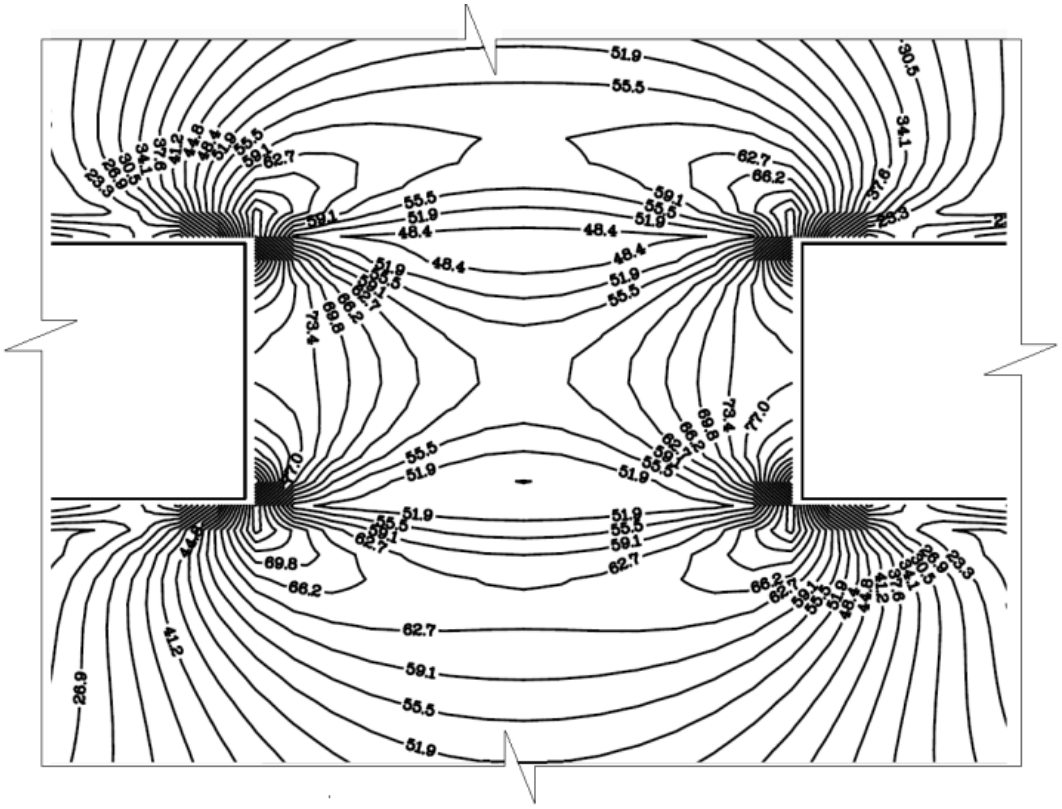

Figure 9. Fragment of isolines of stress T_I in interchamber pillar and corner regions of neighbor chambers for Ω=0°

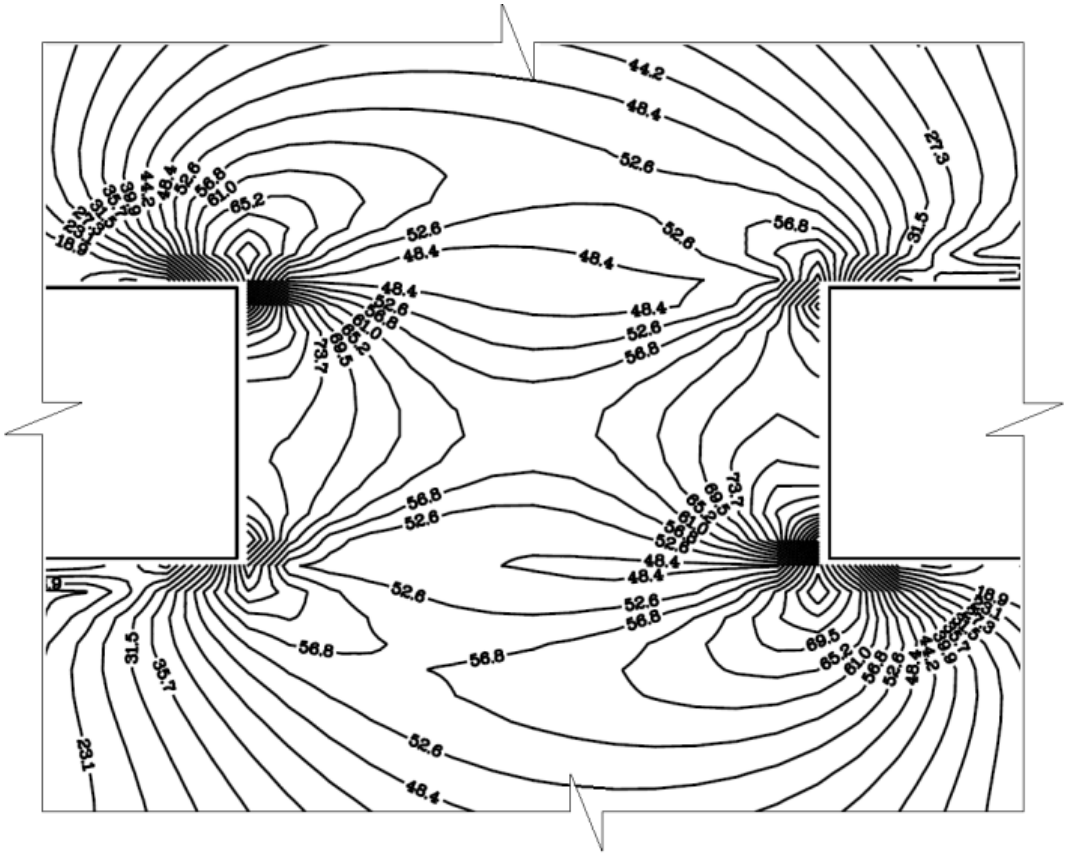

Figure 10. Fragment of isolines of stress T_I in interchamber pillar and corner regions of neighbor chambers for Ω=30°

In case Ω=30° the Barrier pillar I is more loaded than Barrier pillar II, the Roof of chamber 1 more loaded than Roof of chamber 2 and Floor of chamber 2 more loaded than Floor of chamber 1 (Table 6). The stress field of right-upper corner of chamber 2 is cross symmetric to stress field of left-bottom left corner of chamber 2 and so on to stress field of right-bottom corner of chamber 1 and left-upper corner of chamber 2 (see Fig 10).

5. Conclusions

The fundamental solutions of the static problem for elastic plane with arbitrary anisotropic properties are obtained as the sum of residues of complex variable function. The assessment of fundamental solution and their derivatives are presented in closed form. In the distribution space are obtained the regular representations for the Somigliana formulas and the stress calculation formulas. These results are new and represent the subsequent development of the BEM method.

The test results performed for circular hole in anisotropic plane of rhombic system show a higher compliance for the boundary values of displacements and stresses calculated by proposed regular formulas. The results of analysis of the stress-strain state in the vicinity of rectangular mining chambers located in deep from day surface are presented in tables and pictures of isolines.

Acknowledgements

This research is financially supported by a grant from the Ministry of Science and Education of the Republic of Kazakhstan (Grant No. AP05135494).

REFERENCES

[1] Tomlin, G.: Numerical analysis of continuum problems of zoned anisotropic media. Ph.D. thesis, Southampton University (1972).

[2] Brebbia, C., Telles, J., Wrobel L.: Boundary element techniques: theory and applications in engineering. Springer-Verlag, Berlin (1984).

[3] Vable M., Sikarskie D.: Stress analysis in plane orthotropic material by the boundary element method. Int. J. Solids Structures 24(1), 1–11 (1988).

[4] Sun, X., Cen, Z.: Further improvement on fundamental solutions of plane problems for orthotropic materials. Acta Mechanica Solida Sinica 15 (2), 171–181 (2002).

[5] Liu, Y., Huang, L. Sun, X., Cen, Z.: Boundary element analysis for elastic and elastoplastic problems of 2D orthotropic media with stress concentration. Acta Mechanica Sinica 21(5), 472-484 (2005).

[6] Kolosova, E.: Fundamental solutions for anisotropic media and their applications (in Russian). Ph.D. thesis, South Federal University, Rostov-na-Donu (2007).

[7] Hasebe, N., Sato, M.: Mixed boundary value problem for quasi-orthotropic elastic plane. Acta Mech 226(2), 527-545 (2015)

[8] Ding, H ., Jiang, A. Chen, W.: Fundamental solutions for transversely isotropic magneto-electro-elastic media and boundary integral formulation. Science in China Series E 46(6), 607–619 (2003).

[9] Berger, J ., Martin, P., Mantič, V., Gray, L.: Fundamental solutions for steady-state heat transfer in an exponentially graded anisotropic material. Z. angew. Math. Phys. 56, 293–303 (2005).

[10] Schiavone, P., Ru, C.: Integral equation methods in plane-strain elasticity with boundary reinforcement. Proc. R. Soc. Lond. A 454, 2223-2242 (1998).

[11] Szeidl, G., Dudra, J.: Boundary integral equations for plane orthotropic bodies and exterior regions. Electronic Journal of Boundary Elements 8(2) 10-23 (2010).

[12] Zozulya, V.: Regularization of the Divergent Integrals I. General consideration. Electronic Journal of Boundary Elements 4(2), 49-57 (2006).

[13] Lekhnitskii, S.: Theory of elasticity of an anisotropic body. Mir Publishers, Moscow (1981).

[14] Vladimirov V.: Equations of mathematical physics. (in Russian) Nauka, Moscow (1981).

[15] Sh. A. Dildabayev, Sh., Zakir'yanova, G.: Fundamental solutions of the first and second boundary value problems of dynamics for an anisotropic elastic half-plane. (in Russian) Izvestya NAN Respuliki Kazakhstan ser. Fiz.-mat 5, 65-70 (1993).

[16] Lachat JC, Watson JO. Effective numerical treatment of boundary integral equations – formulation for 3-dimensional elastostatics. International Journal for Numerical Methods in Engineering 1976; 10(5): 991-1005.

[17] Clark S.: Handbook of physical constants. Geological Society of America, New Haven (1966).